INTERNATIONAL CONFERENCE ON LIGHTNING PROTECTION
33rd International Conference on Lightning Protection
25 - 30 September 2016
Estoril, Portugal

Methodologies for the charge estimation in the leader corona region used in modeling long air gaps under positive voltage impulses

Oscar Diaz, Vernon Cooray
Lightning Research Group, Division of Electricity
Faculty of Engineering Sciences, Uppsala University
Uppsala, Sweden
oscar.diaz@angstrom.uu.se, vernon.cooray@angstrom.uu.se

Liliana Arevalo
Power Systems HVDC
ABB AB
Ludvika, Sweden
liliana.arevalo@se.abb.com

***Abstract*—Different methodologies have been proposed to represent the physical phenomena taking place in a laboratory electrical breakdown event. The implementation of these methodologies in numerical routines is based in several physical assumptions and a proper calculation of the electrostatic potential distribution. The whole electrical breakdown in air tested with switching-like voltage impulses can be subdivided into three main stages: first, the streamer inception (first corona), then the streamer to leader transition (second corona, leader inception) and the leader propagation. An important element in the last stage is the representation of the leader corona region (streamer region) in front of the leader tip channel as it propagates towards ground. In this paper, with the aid of a finite element method solver to determine the electric potential distribution, two new methodologies to quantify the amount of charge produced in the leader corona region were presented and compared with other ones available in the literature.**

Keywords: high voltage testing; leader type discharge; leader corona region

I. INTRODUCTION

The numerical modeling of electrical gas discharges occurring in atmospheric air due to lightning or electrical transients in power systems have been in continuous development during the last decades in the fields of high voltage techniques and lightning protection. Different methodologies have been proposed to represent the physical phenomena taking place in a complete breakdown, departing both from experimental work and theoretical approaches. The implementation of these methodologies in numerical routines combined with proper physical assumptions and the estimation of the electrostatic potential distribution within a simulation domain give good results compared to the experimental values. The whole electrical breakdown in air tested with switching-like voltage impulses can be subdivided into three main stages: first, the streamer inception (first corona), then the streamer to leader transition (second corona, leader inception) and at last the leader propagation, which would eventually lead to breakdown or withstand of the gap. For the latter, one important element is the representation of the leader corona region (streamer region) in front of the leader tip channel as it propagates towards ground. Most of the authors, use a constant potential gradient required to sustain streamer discharges in a given region in the nearby of the leader tip. Different methodologies for estimating the amount of electric charge from the streamer discharges available to feed the leader channel have been proposed.

In this paper, with the use of a finite element method (FEM) solver to determine the electric potential distribution, two new methodologies to quantify the amount of charge produced in the leader corona region (LCR) were presented and compared with those from other authors. These two new methodologies allows the modeling of complex geometries in three-dimensional domains since the potential distribution is solved in the FEM solver, a powerful tool which is capable to handle almost any geometry.

II. POSITIVE LONG AIR DISCHARGE

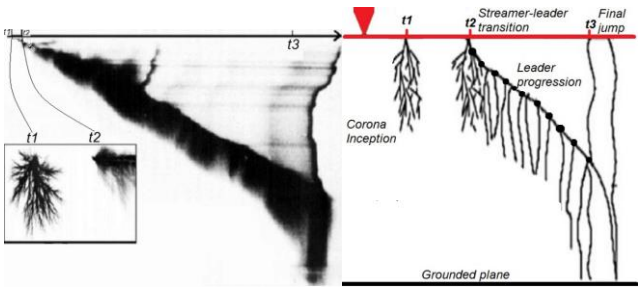

Figure 1. Streak image and schematic representation for the long air gap positive discharge (adapted from [1]).

This work was funded by the divisions of Power Systems HVDC and Power Products – High Power Breakers at ABB AB, Ludvika, Sweden.

The full positive long air gap discharge occurring while testing a rod-to-plane electrode arrangement with positive switching-like voltage impulses can be depicted as it is shown in Fig. 1. The discharge event initiates with the streamer inception at time t_1 (also called first corona). If the electric field increases, it would reach a certain threshold on the electrode surface, increasing at the same time the ionized particles number at the discharge head. Then streamer discharges will start to propagate from a common stem on the electrode. At time t_2 the leader inception takes place (also called second corona or streamer-to-leader transition) after the first streamers have generated enough charge to thermalize the first leader channel segment, raising the channel temperature and electrical conductivity. The LCR feeds charge to the channel at the leader tip; allowing further growth of the channel. The leader tip might cross the air gap until it reaches the grounded plane if the potential gradient in the LCR is high enough to sustain the ionization processes, ca. 450 kV/m for atmospheric air [2]. The final jump condition will happen once the LCR reaches the grounded plane at time t_3. A more detailed work on the long air gap discharge processes description and analysis can be found in [3].

III. Methodologies used for the LCR charge calculation

One common element present in these methodologies is the assumption that to sustain the leader propagation, there should be a constant potential gradient in front of its tip, higher than a certain threshold to permit streamer propagation [4]–[8]. The region or volume that fulfills this assumption is the LCR. A schematic representation of the potential profiles of the positive rod-to-plane discharge along the discharge axis, is presented in Fig. 2.

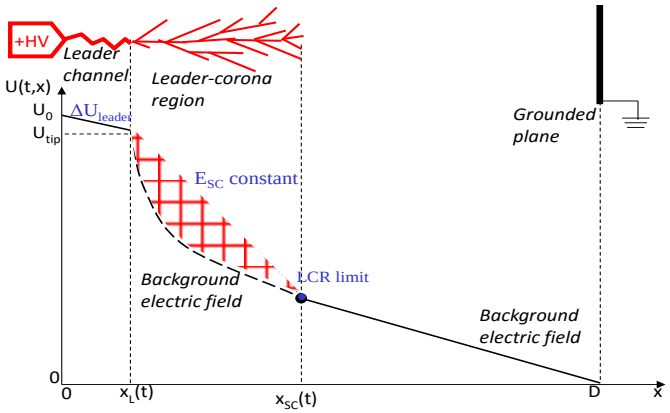

Figure 2. Schematic representation of the potential distribution along the air gap for a rod-to-plane arrangement. Note the grid-shaded region corresponding to the area enclosed by the geometrical potential distribution of the background and the superimposed constant gradient in the LCR

The modified potential profile starting at the leader tip would now have values given by equation (1), which are superimposed to the background potential values to represent the LCR:

$$U_X = U_0 - \Delta U_{leader} - E_{SC}(x_L - dx) \qquad (1)$$

Where U_x is the potential at a distance dx from the leader tip, ΔU_{leader} is the potential drop along the leader channel and E_{SC} is the constant potential gradient in the LCR. The LCR will extend until the LCR limit (streamer front), being the space location where the background potential has the same value as U_X calculated with (1). The main difference among these methodologies resides in the how this LCR potential distribution is represented within the simulation domain potential distribution, and based on that representation, including some additional assumptions, how much net electric charge is in the LCR. In the following subsections, a brief description of some of these methodologies is be presented.

A. *Lalande method*

The method presented in [4], [6] uses the same process to find the LCR limit described in Fig. 2. For the estimation of the LCR charge, the streamers in this region are represented as a cluster of several parallel charge segments, between the leader tip and the LCR limit. For the case of a rod-to-plane electrode arrangement, the amount of charge in the LCR is estimated by finding the area enclosed by the background potential profiles and the superimposed constant potential gradient along the LCR (grid-shaded region in Fig. 2), multiplied by a factor that considers the segment number and geometry.

B. *Charge simulation method (CSM)*

Initially used as a potential distribution calculation tool a few decades ago, it allowed representing symmetric electrode arrangements in a simple way [9-10]. The main idea consists in locating fictitious charges in the vicinity of control points were the potential values is well known. Castelliani used this technique to study the bi-leader discharge [11], representing the LCR in front of the leader tip with a series of charge rings. The total charge enclosed in the LCR is calculated by adding all the individual charge of each ring within the LCR. A general representation of the LCR built from charge rings and potential points is shown in Fig. 3.

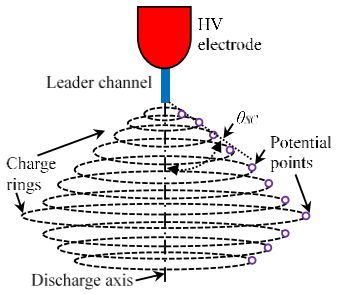

Figure 3. Distribution of the potential points and charge rings for representing LCR in a rod-to-plane configuration using the CSM. Note the symmetrical distribution to the discharge axis of all elements in front of the leader tip.

C. *Becerra method*

An earlier approach considers that the total charge in the LCR can be determined from the difference between the areas enclosed by the geometrical potential distribution of the constant E_{SC} superimposed over the background potential in front of the leader tip, at two successive moments of the leader progression [7] (similar to the grid-shaded region in Fig. 2), multiplied by a constant K_Q, obtained from several different CSM cases. A different more recent approach from the same author, considers the estimation of the streamer charge LCR by solving the Poisson inverse problem by optimization within the LCR [12].

D. *Arevalo method*

This method [8] uses an FEM solver to calculate the electrostatic potential distribution in the simulation domain [13]. This information is compared following the procedure mentioned at the beginning of §2, to determine the electric field lines that fulfill the condition of the constant potential gradient E_{SC} to sustain streamer discharges in the LCR. Then, this region in front of the leader tip with a potential gradient higher than the threshold is divided into *n*- layers. The equivalent electric charge on those layers is calculated estimating the electric flux through a Gaussian surface that encloses each of these layers (2). Thus, the total electric charge inside the LCR is calculated by adding the individual charges dQ_j found for each layer (3):

$$dQ_j = \oint_{Sj} \varepsilon_0 \cdot \vec{E} \cdot \overrightarrow{ds} \tag{2}$$

$$Q_{SC} = \sum_{j=1}^{j=n} dQ_j \tag{3}$$

E. *Single Surface Integral (SSI)*

The method incorporate elements from the previous ones and allows the construction of more complex geometries by using a FEM solver for the electrostatic potential distribution. The LCR is represented by pseudo-electrode rings, whose potentials are assigned following the procedure described at the beginning of §2. Then, all the pseudo-electrodes in the LCR are surrounded by a single closed surface, and the electrical flux is evaluated to estimate the amount of net charge inside (4).

$$Q_{SCtotal} = \oint_{S} \varepsilon_0 \cdot \vec{E} \cdot \overrightarrow{ds} \tag{4}$$

A general view of the geometry elements in the LCR charge calculation for a rod-to-plane electrode arrangement using the SSI is shown in Fig. 4.

F. *Capacitance matrix method (CMM)*

Departing from the same assumptions done while using SSI (§2.E.), CMM also uses a FEM solver for the electrostatic potential distribution in the simulation domain, where the LCR is represented by pseudo-electrode rings with a fixed potential value.

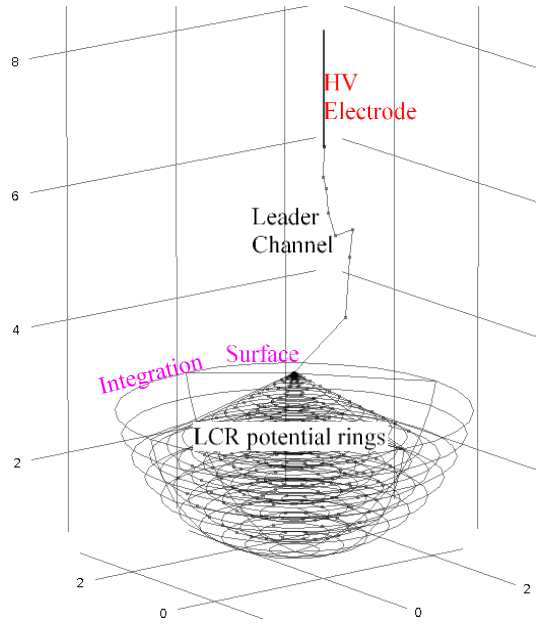

Figure 4. Geometry elements used for the calculation of the LCR using the Single Surface Integral in a 7 m rod-to-plane electrode arrangement. Note the LCR potential rings inside the integration surface.

Departing from the potential distribution solution, the capacitance matrix is calculated for all the pseudo-electrodes and electrodes. This is done by integrating the electrical energy density (W_E) for each *i*-electrode over the simulation domain Ω (5).

$$C_{ii} = \frac{2}{U_i^2} \int_{\Omega} W_E \cdot d\Omega \tag{5}$$

Then, a lineal system with *i*-equations is solved for all known *i*-ring potentials, so all unknown charges Q_i for each ring can be estimated (6).

$$\begin{bmatrix} Q_1 \\ \vdots \\ Q_i \end{bmatrix} = \begin{bmatrix} C_{11} & \cdots & C_{1i} \\ \vdots & \ddots & \vdots \\ C_{i1} & \cdots & C_{ii} \end{bmatrix} \cdot \begin{bmatrix} U_1 \\ \vdots \\ U_i \end{bmatrix} \tag{6}$$

Finally, the total amount of charge in the LCR can be estimated by adding all the individual pseudo-electrode calculated charges (6):

$$Q_{SCtotal} = \sum_{i=1}^{i=k} Qi \tag{7}$$

IV. METHODOLOGIES COMPARISON

Some of the different approaches mentioned in §2 for the LCR charge calculation were analyzed and compared against experimental data, based on their similarity to the LCR representation with potential rings. Among all the experimental data from Les Renardières [14], it is included the electrical charge measured during the streamer inception, also known as first corona. The 10 m rod-to-plane air gap was tested with positive switching-like voltage impulses. The pencil shape electrode diameter was 0.6 m with in a cone-tip in a hemisphere of 0.01 m radius.

The methods of CSM, Becerra, Lalande, SSI and CMM were compared against experimental data. A 2D-axysymmetric model including the electrodes inside a large grounded domain was simulated in the FEM solver [13] to determine the charge at the streamer inception for the electrode arrangement used by Les Renardières [14].

Once simulation was solved and the background electrostatic potential distribution over the simulation domain was known, the pseudo-electrodes for SSI and CMM and potential points for CSM were located and its potential was assigned following (1) and using a value of E_{SC} = 450 kV/m. Then, a new simulation in the FEM solver was done including the pseudo-electrodes for the SSI and CMM and finally the charge in the LCR was calculated.

An important parameter for the CSM, SSI and CMM is the semiangle θ_{SC} (see Fig. 3). It limits the analyzed spatial region/volume starting at the electrode tip until the LCR limit, where the condition of the constant potential gradient to sustain streamers E_{SC} is fulfilled. This value was modified between 60° and 105°, following what was found in [12], [15] for the measured and simulated positive streamer in atmospheric air. For the Lalande [4], [6] and Becerra [7] methods, the geometrical potential distribution along the discharge axis was the only input from the background potential distribution. The electrode potential was fixed to a value ca. 200kV to have on the electrode surface an electric field intensity between 6.5 and 1.1 MV/m.

V. RESULTS AND DISCUSSION

The results for the charge at the streamer inception for the analyzed methodologies following the procedure described in § IV, are presented in Fig. 5.

Since the results for the CMM and SSI originate from the same potential distribution calculated in the FEM solver, the values estimated from both methods differed less than 0.1% between each other; so they were plotted as a single data point in Fig. 5.

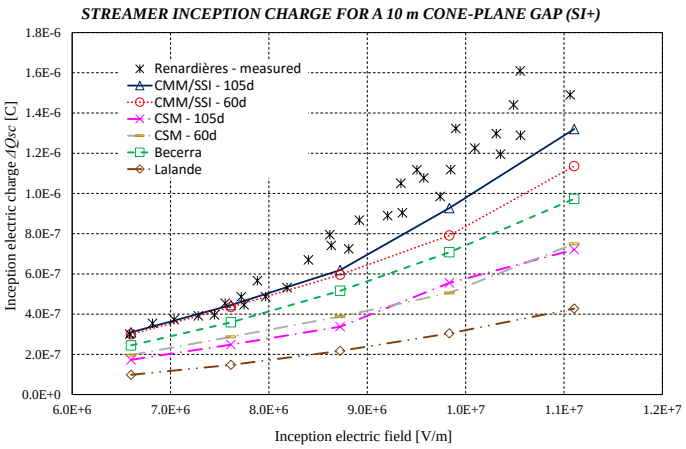

Figure 5. Results from the comparison between different methodologies for the estimation of the electric charge at the streamer inception and a 10 m cone-to-plane air gap tested with switching impulses [14]

As it can be seen, the better accuracy between the simulated values and the measured ones, was found for the larger θ_{SC} in the CMM and SSI, in accordance with the conclusions of [12], where the angle θ_{SC} was modified between 15 and 120° and it is seen that the charge estimations became almost angle independent for larger values of θ_{SC}.

For the CSM, it should be mentioned that the geometry modeling included only the electrode, the potential rings, and their image below to replicate the ground plane. The outer grounded shell that delimits the simulation domain in the FEM solver was not included in the CSM geometry, which might cause their smaller value compared with the experimental values. In the case of the Lalande model, there were geometric parameters to describe the streamer segments like segment width, number and the space between them; that were fixed at 50 µm, 1000 and 25 µm. A different set of this geometric values might give a value closer to the measurements.

VI. CONCLUSIONS

Different methodologies for the calculation of the streamer charge were mentioned and compared. A common element between them is the assumption of a constant potential gradient E_{SC} in the LCR. Two new methodologies SSI and CMM were proposed, based on the electrostatic potential distribution obtained while representing the LCR as a cluster of ring pseudo-electrodes. Representing the LCR in the form of potential rings permits the easy use of SSI and CMM on non-symmetric geometries, like a tortuous leader channel or electrodes with protrusions.

A difference lower than 0.1% was found between this new methodologies since they both depart from the estimation of the potential distribution done by the FEM solver. Good agreement was found between both CMM/SSI and the measured values for the larger values tested for θ_{SC}.

All the methodologies mentioned for the LCR charge estimation include geometrical adjustment constants that might

influence the result. This effect was seen while assigning the location for the potential rings and pseudo-electrodes in the CSM and SSI-CMM. Two variables that could be modified while assigning the LCR ring location were the angle step chosen to cover θ_{SC} and the increasing distance between different radial locations to have a better detail in the electrode vicinity.

REFERENCES

[1] A. Castellani, A. Bondiou-clergerie, P. Lalande, A. Bonamy, and I. Gallimberti, "Laboratory study of the bi-leader process from an electrically floating conductor. Part 2: Bi-leader properties," *IEE Proc. - Sci. Meas. Technol.*, vol. 145, no. 5, pp. 193 – 199, 1998.

[2] O. Diaz, L. Arevalo, and V. Cooray, "Leader channel models for long air positive electrical discharges," *J. Electrostat.*, vol. 76, pp. 208–215, 2015.

[3] I. Gallimberti, "The mechanism of the long spark formation," *Le J. Phys. Colloq.*, vol. 40, no. C7, pp. C7–193–C7–250, 1979.

[4] P. Lalande, "Etude des conditions de foudroiement d'une structure au sol," Universite de Paris XI ORSAY, 1996.

[5] A. Bondiou-Clergerie and I. Gallimberti, "Theoretical modelling of the development of the positive spark in long gaps," *J. Phys. D. Appl. Phys.*, vol. 27, pp. 1252–1266, 1994.

[6] N. Goelian, P. Lalande, A. Bondiou-Clergerie, G. L. Bacchiega, A. Gazzani, and I. Gallimberti, "A simplified model for the simulation of positive-spark development in long air gaps," *J. Phys. D. Appl. Phys.*, vol. 30, no. 17, pp. 2441–2452, 1997.

[7] M. Becerra and V. Cooray, "A simplified physical model to determine the lightning upward connecting leader inception," *IEEE Trans. Power Deliv.*, vol. 21, no. 2, pp. 897–908, 2006.

[8] L. Arevalo, D. Wu, and B. Jacobson, "A consistent approach to estimate the breakdown voltage of high voltage electrodes under positive switching impulses," *J. Appl. Phys.*, vol. 114, no. 8, p. 083301, 2013.

[9] H. Singer, H. Steinbigler, and P. Weiss, "A charge simulation method for the calculation of high voltage fields," *IEEE Trans. Power Appar. Syst.*, vol. 93, no. 5, pp. 1660–1668, 1974.

[10] N. H. H. Malik, "A review of the charge simulation method and its applications," *IEEE Trans. Electr. Insul.*, vol. 24, no. 1, pp. 3–20, 1989.

[11] A. Castellani, "Calcul du champ electrique par la methode des charges equivalentes pour la simulation d'une decharge bi-leader," 1995.

[12] M. Becerra, "On the estimation of the charge of positive streamers propagating in air," *IEEE Trans. Dielectr. Electr. Insul.*, vol. 21, no. 2, pp. 627–634, 2014.

[13] "COMSOL multiphysics user guide (Version 5.1)," *COMSOL, AB*, 2015.

[14] Les Renardierès Group, "Research on Long Air Gap Discharges at Les Renardières - 1973 results -," *Electra*, vol. 35, pp. 49–156, 1974.

[15] P. Ortéga, F. Heilbronner, F. Rühling, R. Díaz, and M. Rodière, "Charge–voltage relationship of the first impulse corona in long airgaps," *J. Phys. D. Appl. Phys.*, vol. 38, no. 13, pp. 2215–2226, Jul. 2005.